MEMS Mega-pixel Micro-thruster Arrays for Small Satellite Stationkeeping

Daniel W. Youngner[(1)], Son Thai Lu[(1)], Edgar Choueiri[(2)], Jamie B. Neidert[(3)], Robert E. Black III[(3)], Kenneth J. Graham[(3)], Dave Fahey[(4)], Rodney Lucus[(4)], Xiaoyang Zhu[(5)]

(1) Honeywell Technology Center, 12001 State Hwy 55, Plymouth, MN 55441, 763-954-2773, youngner_dan@htc.honeywell.com. . (2) Princeton University Electric Propulsion and Plasma Dynamics Lab (EPPDyL), Princeton, NJ. (3) Atlantic Research Corporation, Gainesville, VA. (4) Quantic Industries, Hollister, CA. (5) University of Minnesota Chemistry Dept., Minneapolis, MN.

Abstract. Small satellites flying in clusters require periodic "stationkeeping" to keep them in place. The required impulse is very small – the goal is not to keep the individual satellites in rigid formation, but only to keep them in well-defined orbitals with respect to one another. The necessary impulse, therefore, is only the amount needed to overcome the difference in drag between the most-affected and the least-affected satellites in the cluster. Estimates are that the differential drag can be overcome by providing ~1 μNsec (micro-Newton second) to ~1 mN sec (milli-Newton second) every 10 to 100 seconds throughout each satellite's mission. The system we are developing will do that. The thrusters have very low power and energy thresholds for ignition (~10 mWatts, ~100 μJoules), and no moving parts so they are expected to be highly reliable. A single thruster array contains a quarter of a million separate thrusters.

Background

There is interest within the satellite community in replacing single large satellites with clusters of smaller satellites[1-4]. Each satellite in a cluster might be as small as a deck of playing cards, but collectively the cluster could function like a single satellite equal in size to the diameter of the cluster – hundreds or even thousands of meters across. Building a cluster of small satellites can be cheaper and more versatile than building a single large one. Additionally, a cluster can be more robust than a single large satellite; if one part fails another can be maneuvered into its place and take over its function.

Some space missions would be virtually impossible without satellite clusters. NASA has a program called the "Astronomical Search for Origins[5], for example." In it, NASA wants to image distant planets using the ~1 millimeter characteristic wavelengths of water and organic molecules. The premise is that if a planet's atmosphere contains the precursors for life (water and organics), there's a chance that the planet will contain some form of life. To image a planet that subtends an arc (θ) of less than 1E-7 radians using wavelengths (λ) of ~1mm, one needs an aperture that's λ/θ, or ~10km across. That's way too big to be built as a conventional single-satellite imaging system. It is, however, plausible that such a system could be built from a cluster of microsatellites. Figure 2 shows how such an imaging system, using variable true optical delays[6,7] at the nodes defined by each satellite, might look.

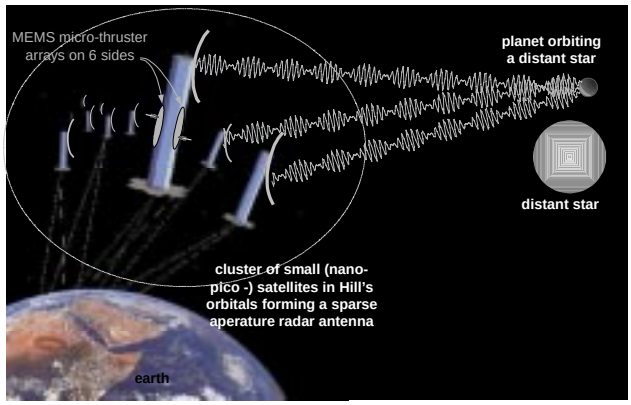

Figure 1: Cluster of microsatellites being used to image a distant planet.

There are significant challenges to getting clusters to work, however. One challenge results from the fact that the satellites in a cluster don't stay put – they continually move about with respect to one another. In theory the individual satellites can be made to orbit one another in "Hill's orbitals[2]." Hill's orbitals are orbits the individual satellites make with respect to the center of mass of the cluster as the cluster orbits the earth. Hill's orbitals are complex, but they are well defined. Figure 2 shows Hill's equations expressed in the reference frame of the cluster, and the orbits that satisfy those equations.

Unfortunately, the real-world problem is more complex than the solutions to Hill's equations might lead one to believe. In the real world the individual satellites experience atmospheric drag and perturbing forces due to non-idealities of the earth's gravitational

field, luni-solar gravity, and solar radiation pressure[8]. All of these perturbations affect the different satellites in a cluster differently. To keep them in their prescribed Hill orbital, each satellite requires periodic corrections to its orbital position and orientation; each satellite requires periodic "stationkeeping".

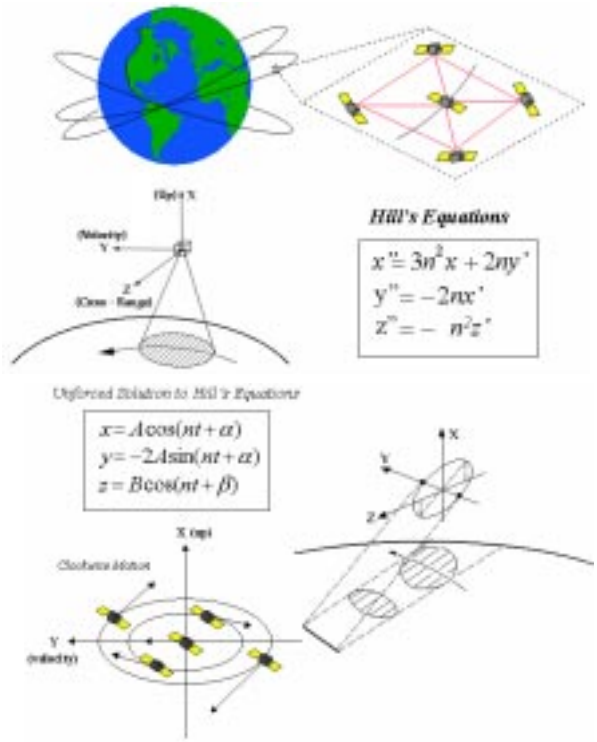

Figure 2: Hill's equations and their solutions[2].

The system we are developing will provide the necessary impulse to do that stationkeeping.

Our Approach

Figure 3 shows a schematic of a single thruster in our system. A MEMS thruster array contains a quarter of a million separate thrusters on a 1.3" x 1.3" silicon die; the thrusters themselves are laid out one a 512 by 512 grid with 51μm by 51μm pitch. Each thruster has its own heater filament which is co-axially aligned to a hollow fuel-filled cavity directly above it. The filaments are built monolithically on top of space-qualified RICMOS® electronics, so each thruster is individually addressable and ignitable.

We've selected two-stage approach to detonating the fuel and creating thrust. In stage 1 a small (~1 nanogram) charge of thermally-detonatable lead styphnate is heated to its auto-ignition temperature (270˚C). The styphnate explodes, releasing a lot of energy but not a lot of usable momentum. In stage 2 the exploding styphnate ignites a nitrocellulose mixture in the overhead cavity. A special nitrocellulose mixture has been chosen in which the propagation speed of the shock wave through the fuel is rapid, yet the burn rate of the fuel is relatively slow. The intent is that the shock front propagates through the nitrocellulose more quickly than the burn-products are created and expelled – so quickly in fact, that the entire volume of shock-heated propellant in a pixel is converted to gas virtually instantaneously and expelled as a gas. The design shown in Figure 3 includes an optional egress channel. In our first attempt at building these structures we have opted to omit the egress channels.

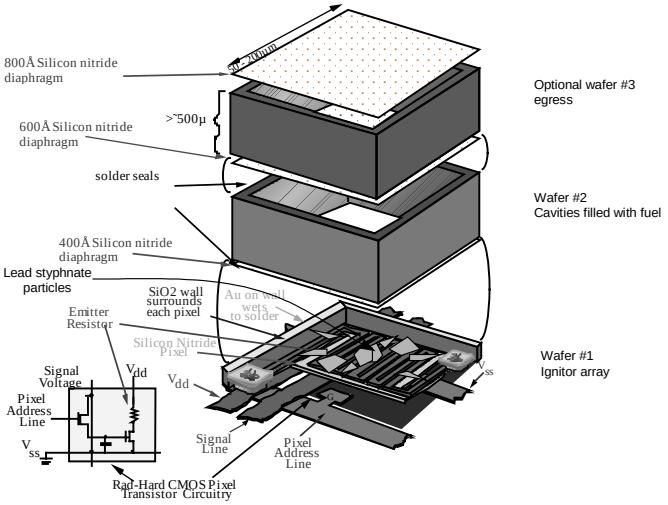

Figure 3: Schematic of a single pixel in the mega-pixel array we are building.

Modeling

Before the structures can be built they first have to be modeled. An explosion in one cavity should not shatter the walls of that cavity, nor should it cause the fuel in neighboring cavities to ignite. Mechanical shock and thermal shock are both expected to be significant, and extensive modeling is needed to insure that the structures behave as envisioned.

Figures 4, 5 and 6 show ANSYS simulations of how the cavities are stressed when the fuel in one of the cavities is ignited and a 100-atmosphere (1E8 dynes/cm2, or 10MPa) pressure is temporarily created. The plots are for cavities with a pitch of 50 microns, a wall thickness of 10 microns, and a radius

of curvature at the corners of 10 microns. Other simulations with different input parameters show similar results. The stress values are in dynes/cm2, with negative values depicting compressive stress and positive values depicting tensile stress. Note from Figures 4 and 5 that the tensile stresses is greatest at the corners. The maximum stress is a strong function of both the wall thickness and the radius of curvature of the corners. Note from Figure 6 that a 100-atmosphere pressure causes the walls to flex by only 60 nanometers – a small enough amount that both stress and strain will scale nearly linearly with pressure over the entire pressure range and cell size of interest.

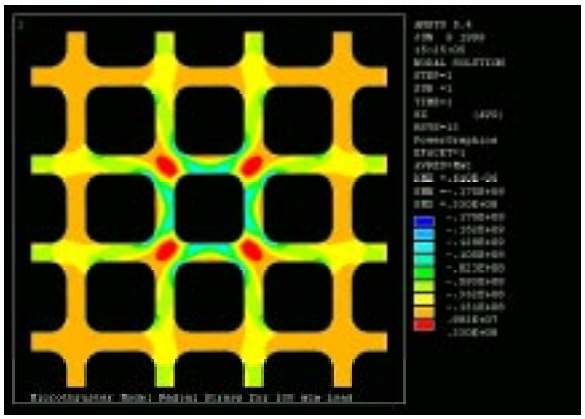

Figure 4: Radial stress in Pixel sidewalls when the internal pressure in one cavity is 100 atmospheres.

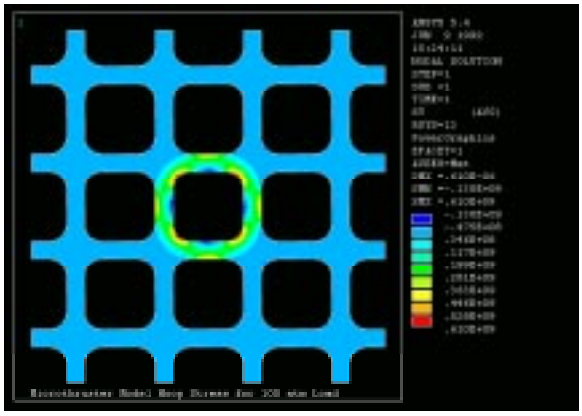

Figure 5: Hoop (tangential) stress in the pixel sidewalls when the internal pressure in the cavity is 100 atmospheres.

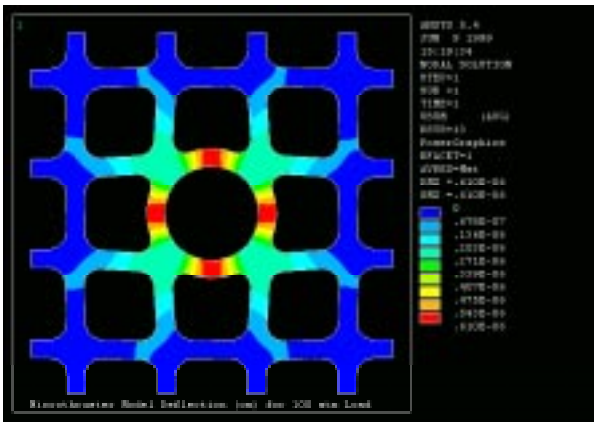

Figure 6: Wall deflections when a 100 atmosphere explosion occurs in a cavity, magnified 1000x.

Micro-machined silicon can withstand tensile stresses of up to ~1 GPa (1 E10 dynes/cm2 or 10,000 atmospheres) depending on the micro-roughness of the wall edges, adsorbed water on the surface, and a host of other factors[9]. Figure 5 shows what are considered to be "safe" regions of parameter space – regions where the fuel in a cell could be ignited without significant risk that the walls will crack or that the fuel in neighboring cells would be ignited parasitically by the explosions.

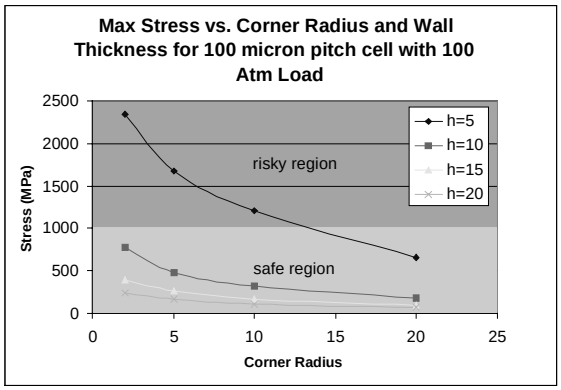

Figure 7. Maximum wall stress for various radii of curvature and wall thickness (h) when a 100-atmosphere explosion occurs in a pixel. The cell pitch in these simulations is 100 microns x 100 microns.

Our designs (see Figure 3) include silicon nitride diaphragms that separate the styphnate-coated filaments from the fuel-containing cavities. The diaphragms must be strong enough not to rupture when the fuel is loaded into the cavities, but weak enough to break and allow the explosion to propagate when the styphnate is ignited. Guided by simulations in Ohring's book[10], we modeled the diaphragm rupture

strength for a variety of designs. As shown in Figure 8, it is possible to have diaphragm rupture strengths from ~1 atmosphere to several hundred atmospheres using reasonable film thickness and diaphragm radii.

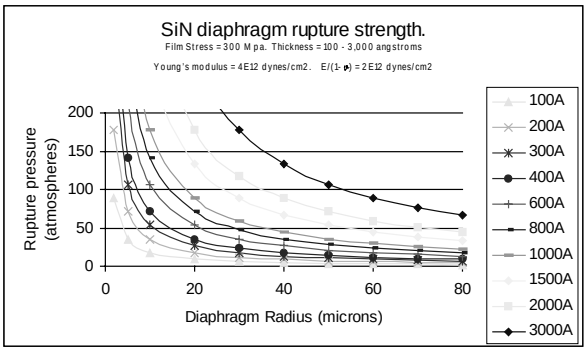

Figure 8: Modeled SiN Diaphragm rupture strength for radii from 2 microns to 80 microns, and thicknesses from 100 angstroms to 3000 angstroms.

Design & Layout

We designed and laid out 22 variations of the thruster on a single mask set. The designs include cavity diameters ranging from 41 μm to 143 μm, corner radii of curvature from 2 μm to 71.5 μm, wall thickness from 10 μm to 41 μm, and diaphragm thickness from 30 nanometers to 200 nanometers. The more aggressively designed structures were laid out with wide SiO2 "firewalls" after 18 repeats of the cells so that if one cell were to go off and inadvertently ignite its neighbor, which would ignite its neighbor, ... the domino effect would terminate after at most 18 cells. Figure 9 shows a portion of the layout.

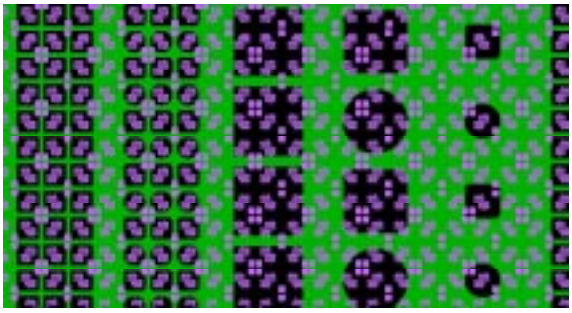

Figure 9: Layout of the cells.

Processing

Building the structures entails several sub-projects including: 1.) processing the igniter wafers, 2.) building walls around the individual igniters, 3.) coating the filaments with a Self-Assembled Monolayer (SAM) to facilitate preferential deposition of lead styphnate on the filaments, 4.) preparing and applying the lead styphnate igniter suspension to the igniter filaments, 5.) creating the hollowed-out cavity wafers, 6.) bonding the styphnate-coated filament wafers to the cavity wafers, 7.) mounting the 2-layer structures onto appropriate packages, and 8.) loading the cavities with fuel. Each of those steps is described in greater detail in the paragraphs below:

1.) ***Igniter wafers:*** Honeywell has been making and selling infrared scene projectors since 1989[11,12]. As scene projectors, the various pixels in a 512 x 512 array are heated to create synthetic infrared scenes. The scene projectors function like flat-panel TV's, but instead of emitting visible light, the pixels emit heat. For this program the pixels will be addressed individually and will be used to ignite individual thruster cells. The pixels have resistances of from 21kΩ to 126kΩ. When turned on they reach temperatures of up to 1100° Kelvin in about 10 msec. The wafers contain rad-hard RICMOS® underlayer electronics to enable row-column addressing with RS-232 protocol. A complete description of the design and process involved in making the igniter wafers can be found elsewhere[11,12]. Figure 10 shows an optical photograph of a 4" silicon wafer containing four (4) 512 x 512 arrays, eight (8) 128 x 128 arrays, and a handful of smaller test structures. Figures 11 and 12 respectively show an optical blow-up of one the interior of the array, and a SEM of a single heater pixel.

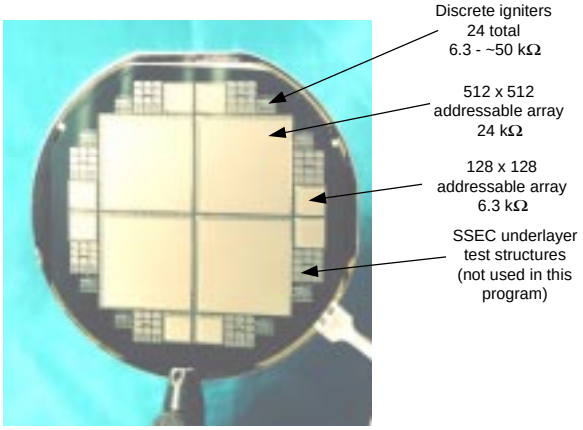

Figure 10: Optical photo of igniter wafer.

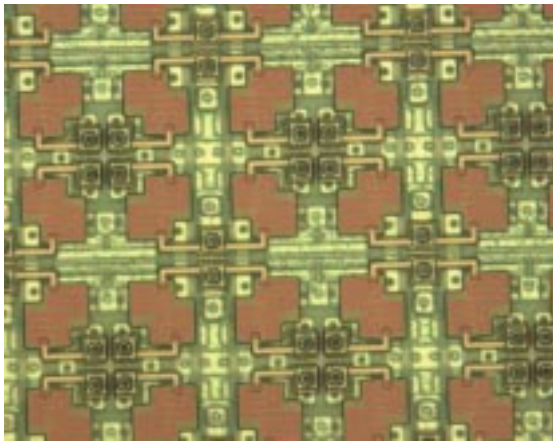

Figure 11: Optical photo showing ~20 of the 262,144 igniter filaments in an array.

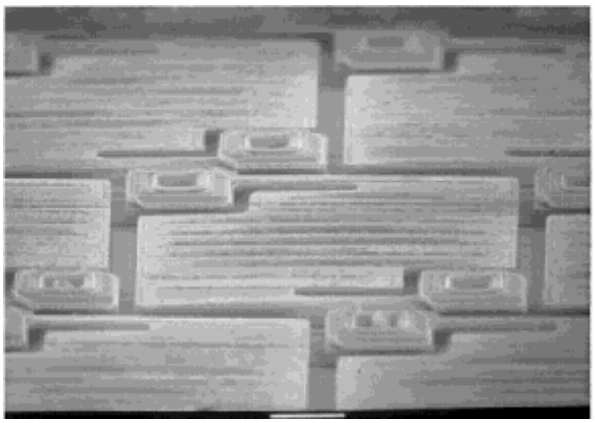

Figure 12: Close-up SEM of an addressable heater filament. Magnification = 1350x.

2.) ***Building walls around individual pixels:*** Five micron (5μ) high walls were built around the igniter filaments, and the tops of the walls were coated with gold. Gold was chosen because it bonds well to the solder which will be applied to the bottoms of the cavity wafers. Figure 13 shows a test pixel with a 50 micron diameter cavity surrounding a single pixel. The SiO2 walls surrounding the filament are a minimum of 40 microns thick, ensuring that even if the explosion in the pixel is much more energetic than modeled, the walls will not fracture.

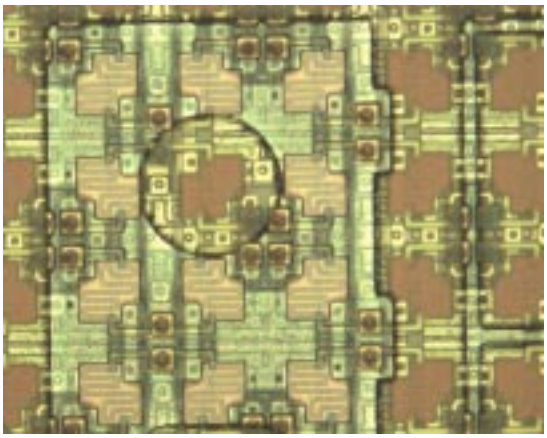

Figure 13: Optical photo showing a circular cavity and SiO2 wall around a single igniter filament.

3.) ***Applying SAM:*** Were we to apply the lead styphnate detonator material directly to the wafer, the styphnate would stick not only to the filaments (which we do want) but also to the gold on top of the SiO2 walls (which we don't want). A Self-Assembled Monolayer (SAM) of dodecanethiol was preferentially formed on the Au surface by immersing the wafer in a 0.5 millimolar solution of dodecanethiol in iso-octane. The SAM reduces surface energy on gold, thereby preventing water wet-ability and insuring that the lead styphnate suspension would wet only the filaments. All indications are that this process step worked well.

4.) ***Applying the detonator to the filaments:*** A water-based suspension of sub-micron particles of lead styphnate was prepared by milling a bulk sample very slowly for a very long time (96 hours mill time to collect 2.6 grams). The mixture was puddle-coated onto the igniter wafer, partially dried, then lightly swabbed with foam pads to remove the excess. As shown in Figure 14, the styphnate particles settled predominantly on the filaments with very little adhesion to the gold. We estimate that the lead styphnate is, on average, about 1 micron thick.

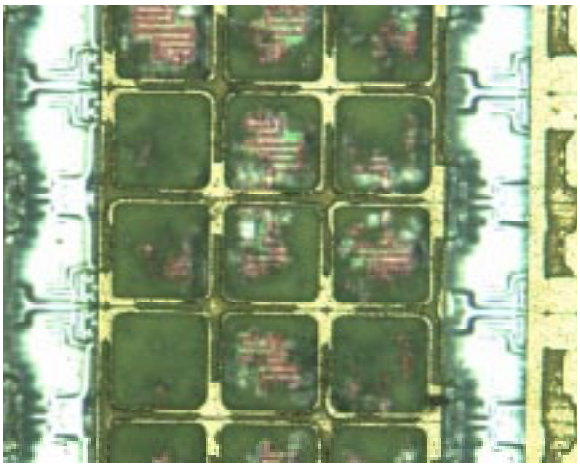

Figure 14: Optical photo of filaments coated with lead styphnate.

5.) ***Creating the co-axially aligned cavities:*** Doubly-polished silicon wafers had thin silicon nitride diaphragms deposited on one side and cavities etched all the way through from the other side. A thin solder layer was deposited on the silicon nitride around each diaphragm and patterned so that the solder would line up with the gold on the igniter wafers. Figure 15 shows a SEM cross-section of the cavity wafer. The various shapes and sizes of the cavities can be seen in the figure.

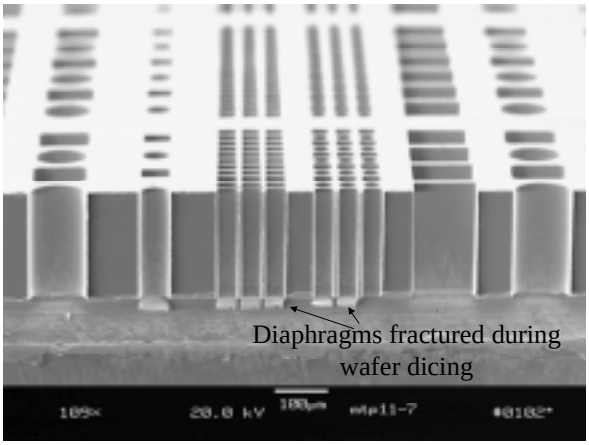

Figure 15: Cavities that will get filled with fuel. Magnification = 70x.

6.) ***Wafer-to-wafer bonding:*** The styphnate-coated igniter wafer and the cavity wafer were aligned to one another and placed in a heated vacuum chamber overnight. After sufficient outgassing the two-wafer structure was heated to 180˚C (the reflow temperature of the solder) and the wafers were pressed together. After cooling the wafer was partitioned into a set of discrete die.

7.) ***Packaging:*** Custom circuit boards were designed and built to accept the MEMS thruster die. The boards, when populated with drive and addressing electronics, enable addressing and ignition of individual pixels through an RS-232 serial port. Figure 16 is an optical photo of a packaged 512 x 512 die.

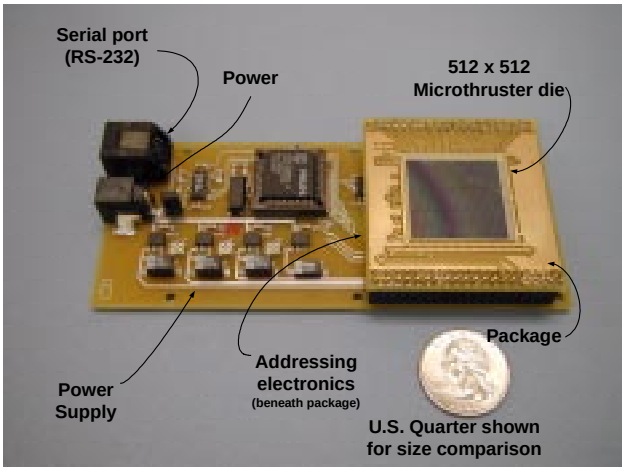

Figure 16: Optical photograph of a bonded microthruster.

8.) ***Filling the cavities with fuel:*** The board-mounted microthruster die were shipped to the Atlantic Research Corporation (ARC) for loading with a gas generator composition – in this case an unfilled double-base solid nitrocellulose propellant. Since the cavities are very small, getting the propellant to go all the way to the bottoms of the cavities is a challenge. Figure 17 shows the system we are using to load the propellant. The entire cavity-filling process is done under vacuum on a temperature controlled plate.

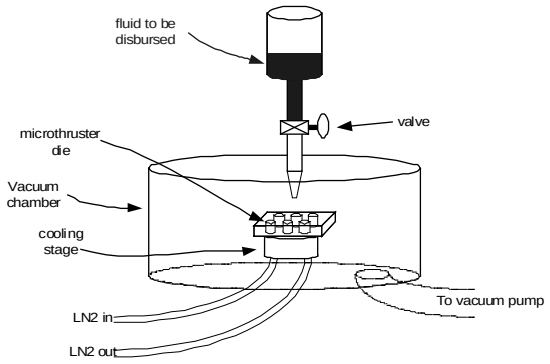

Figure 17: Schematic of the system used at ARC to fill cavities with propellant.

Testing

The thrust measurements will be conducted at Princeton University's Electronic Propulsion and Plasma Dynamics Lab (EPPDyL) micropropulsion research facility, which was recently built under a DURIP grant from AFOSR. It consists of a large (8-foot diameter and 24-foot long) dielectric (fiberglass) vacuum tank in which a vacuum level of 10^-5 torr will be maintained during the proposed experiments. The 48-inch diffusion pump for this facility has a pumping rate of 120,000 l/s and will be operated under an actively cooled trap maintained at a temperature below -75° C by a liquid nitrogen cooling system thus insuring no pump oil contamination to the experiment. It is backed up by a 3000 cfm mechanical pumping subsystem.

The most critical measurement is that of the impulse bit. It will be made using EPPDyL's new microthrust stand which is an improved version of the laboratory's older "swinging gate" thrust stand used in many previous studies[13]. The new thrust stand is almost identical to the one recently built by EPPDyL for NASA-JPL's micropropulsion laboratory which can resolve 20 μNs impulses. The impulse bit is obtained form the recorded dynamics of the thrust arm whose position is measured with a laser interferometric proximeter system (IPS) developed at EPPDyL under funding from NASA-JPL and AFOSR. It is shown schematically in Figure 18, and yields a position measurement with a 10 nm accuracy.

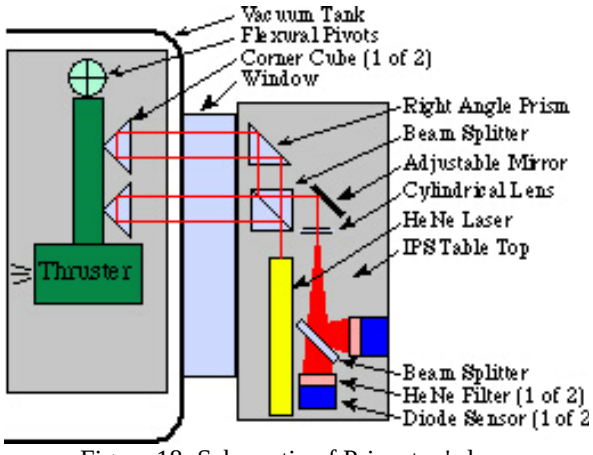

Figure 18: Schematic of Princeton's laser interferometric proximeter system (IPS).

As this paper is being written, the structures are at ARC and are being filled with fuel. Accordingly we don't yet have performance data to report. Based on modeled performance, however, we anticipate results as shown in table 1 below.

Table 1: Anticipated performance of the MEMS mega-pixel microthruster array.

Attribute	Expected Value
Mass of fuel per pixel	0.5 - 8 μg
Number of pixels per array	up to 262,144
Total mass of pixel array, including fuel	2.4 gm
Specific Impulse (Isp)	100 - 300 seconds
Impulse per pixel	0.5 - 20μ Nt sec
Power to ignite a pixel	~10 mWatt
Energy to ignite a pixel	~100 μJoule

Summary

In this paper we reported on a MEMS Mega-pixel micro-thruster array designed for stationkeeping of small satellites. The goals of the project included (1) modeling the mechanical and thermal properties of the structures, (2) building the micro-thruster arrays, (3) measuring the performance of the thrusters using Princeton EPPDyL's new micro-thruster stand, and (4) generally advancing the fundamental understanding of how explosions occur in very small structures.

Acknowledgements

This work was sponsored by AFOSR Contract #F44620-99-C-0012, Dr. Mitat Birkan contract monitor.

We are indebted to Dr. Bill Herb for help with the simulations, to Mr. Dane Larson for help with processing, and to Mr. Tom Rezachek for help with the electronics.

References

1.) Air Force Research Laboratory, Formation Flying & Micro-Propulsion Workshop, 20-21 October 1998, Edwards AFB California, Dr. Ronald A. Spores, et. al.

2.) Captain R. Cobb, “TechSat 21 Advanced Research and Technology Enabling Distribute Satellite Systems”, Proceedings of the Air Force Research Laboratory, Formation Flying & Micro-Propulsion Workshop, Edwards AFB California, 20-21 October 1998.

3.) D. H. Lewis, program manager. "Microsatellite Propulsion and Attitude Control System", http://www.design.caltech.edu/micropropulsion. Project Title: DARPA BAA 96-19.

4.) http://quark.plk.af.mil/vsd/techsat21.

5.) http://www.jpl.nasa.gov/sespd/space/astro.html

6.) D. Baldwin, "Optical True Time Delay for Wideband Optical Transmission Systems", Proceedings of the Sixth Annual ARPA Symposium on Photonic Systems for Antenna Applications, PSSA-6, 5-7 March 1996, Monterey, California.

7.) D. Baldwin "Optical Communications in Satellites", Scientific Honeyweller, Communications Issue, Vol. 11 no. 1, Fall 1991.

8.) R. Sedwick, E. Kong, & D. Miller “Exploiting Orbital Dynamics and Micropropulsion for Aperture Synthesis Using Distributed Satellite Systems: Applications to TechSat21” Proceedings of the Air Force Research Laboratory, Formation Flying & Micro-Propulsion Workshop, Edwards AFB California, 20-21 October 1998.

9.) Sensors & Actuators,Vol 20,#1&2, 1989, p. 124.

10.) M. Ohring, The Material Science of Thin Films, Academic Press, New York, 1992. page 410.

11.) B. Cole, R. Higashi, et. al., “512 x 512 Cryovacuum Resistor Infrared Scene Projector”, Proceedings of the SPIE, Orlando, FL, 1996, Vol. 2469.

12.) B. Cole, R. Higashi, et. al., “512 x 512 WISP (Wide Band Infrared Scene Projector) Arrays”, Proceedings of the SPIE, Orlando, FL, 1996, Vol. 2741.

13.) E.A. Cubbin, J. Ziemer, E.Y. Choueiri, and R.G. Jahn. “Laser Interferometric Measurements of Impulsive Thrust”. Review of Scientific Instruments, 68(6): 2339--2346, 1997.